

Ambient-pressure synthesis of single-crystal MgB₂ and their superconducting anisotropy

Y. Machida* and S. Sasaki

Materials and Structures Laboratory, Tokyo Institute of Technology, 4259 Nagatsuta, Midori-ku, Yokohama 226-8503, Japan

H. Fujii

National Institute for Materials Science, 1-2-1, Sengen, Tsukuba 305-0047, Japan

M. Furuyama, I. Kakeya, and K. Kadowaki

Institute of Materials Science, University of Tsukuba, 1-1-1, Tennoudai, Tsukuba 305-8573, Japan

(Received 27 July 2002; revised manuscript received 15 November 2002; published 18 March 2003)

We synthesized single crystalline MgB₂ under ambient pressure by using conventional materials and equipment. The single crystals of MgB₂ were of good quality, where the crystal structure refinements were successfully converged with $R=0.020$. The measurements of the magnetic properties yielded a sharp superconducting transition at 38 K with transition width $\Delta T_c=0.8$ K. The upper critical field for applied field parallel to the ab plane (H_{c2}^{ab}) reveals a positive curvature, while H_{c2} parallel to the c axis (H_{c2}^c) increases linearly in temperature dependence, which yields a temperature dependence of the superconducting anisotropy ratio of $\gamma = H_{c2}^{ab}/H_{c2}^c$ with $\gamma \sim 1$ near T_c and 4.0 at 25 K.

DOI: 10.1103/PhysRevB.67.094507

PACS number(s): 74.25.Bt, 74.25.Ha, 74.62.Bf, 74.25.Op

I. INTRODUCTION

The recent discovery of superconductivity at 39 K in magnesium diboride MgB₂ (Ref. 1) has attracted great scientific interest because of the highest T_c among conventional metals and intermetallic compounds. Several experiments indicated phonon-mediated s -wave BCS superconductivity^{2,3} and the appearance of a double energy gap was predicted.^{4,5} Specific heat⁶ and spectroscopic⁷ measurements, scanning tunneling spectroscopy,^{8,9} gave evidence of this prediction. However, several key parameters such as the upper critical fields H_{c2} and their anisotropy ratio γ , the magnetic penetration depth λ , the coherence length ξ and Ginzburg-Landau parameter κ are not well established because of the difficulty of growing high quality MgB₂ single crystals.

In particular, the anisotropy ratio $\gamma = H_{c2}^{ab}/H_{c2}^c$ is important to characterize superconducting properties and for applications of MgB₂. Here H_{c2}^{ab} and H_{c2}^c are the in-plane and out-of-plane upper critical fields, respectively. The reported γ values vary widely depending on the measurement methods or on the sample types. The values determined from resistivity on polycrystals,¹⁰ aligned crystallites,¹¹ c -axis oriented films,¹²⁻¹⁴ and single crystals¹⁵⁻²³ have been reported to be 6-9, 1.7, 1.3-2, and 2.6-3, respectively.

So far, there have been several reports on superconducting properties in MgB₂ single crystals.^{15,17,18,24} Most of these crystals were synthesized under high pressure, typically 5 GPa, with high pressure facilities. Shapes of crystals grown under high pressure are mostly irregular, so that it is almost impossible to recognize the correspondence between the crystal shapes and crystallographic axes. This causes experimental difficulties for measurements on anisotropic properties.

In this paper, we report on a method to grow a single crystal under ambient pressure, which does not require special equipments. Then we characterize the crystals in various ways. The grown crystals shows good crystallographic quali-

ties compared with crystals grown under high pressure in the literature,^{15,24} and the correspondence between sample edges and crystallographic axis is not hard to recognize. Using these crystals, we investigated the superconducting properties through magnetization measurements, and found that the anisotropy parameter γ of H_{c2} strongly depends on temperature, in particular just below T_c .

II. AMBIENT PRESSURE SYNTHESIS AND CHARACTERIZATION

The single crystals were grown in the stainless (SUS304) tube. Typical dimensions of stainless tubes are 32, 1.5, and 110 mm for the outer diameter, the wall thickness, and the length, respectively. The inner surface of the tube was sealed by Mo sheet (99.95%, Nilaco Co.) with the size of 0.05

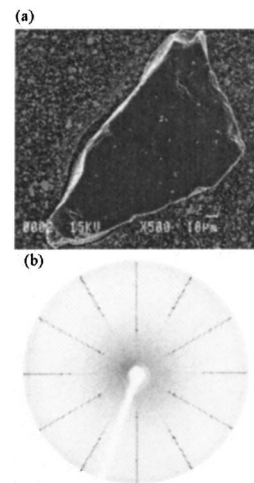


FIG. 1. (a) SEM image of a MgB₂ single crystal with a size of about 100 μm . (b) X-ray precession photograph of the single crystal.

TABLE I. Structural parameters of single crystals. Lattice constants: $a=b=3.0863(4)$ Å, $c=3.5178(4)$ Å. Agreement factors: $R=0.020$, $R_w=0.027$ (w =weight).

Atom	atomic orientation	U_{11} (Å ²)	U_{33} (Å ²)	B_{eq} (Å ²)
Mg	(0,0,0)	0.0078(2)	0.0054(2)	0.382(2)
B	(1/3,2/3,1/2)	0.0068(2)	0.0058(2)	0.371(2)

$\times 100 \times 200$ mm³ to avoid direct reaction between the container materials and Mg/B materials. One end of the SUS304 tube was pressed with a vise and sealed in an Ar gas atmosphere by arc welding. The starting materials of a B (99.9%, Furuuchi Chemical Co.) chunk with the size of 3~5 mm and a Mg (99.99%, Furuya Metal Co.) chunk, which was cut out with the size of about 1 cm³ from Mg block, were filled inside the tube. Then the other end of the tube was pressed with a vise and sealed in an Ar gas atmosphere by arc welding, as well. For crystal growth, the temperature of the furnace inside, which the crucible was put, was raised from room temperature to 1200 °C for 40 min. The single crystals finally obtained were about 100–300 μm, which had a partly hexagonal shape with a shiny golden color when observed under an optical microscope.

The single crystal images observed by a scanning electron microscope (SEM) is shown in Fig. 1(a). The crystals were found to have very flat surfaces. The structural analysis was carried out using a x-ray precession camera, a four-circle diffractometer, and a transmission electron microscope (TEM). The x-ray precession photograph indicated that the crystal has a hexagonal structure, as shown in Fig. 1(b). The diffraction data were collected by using graphite monochromated MoK_α radiation at room temperature, and refined by the least-square procedure using 86 reflections as the average of the measured 866 reflections. Finally, we obtained structural the parameters as shown in Table I.

To confirm the structure of the MgB₂ phase, we took a

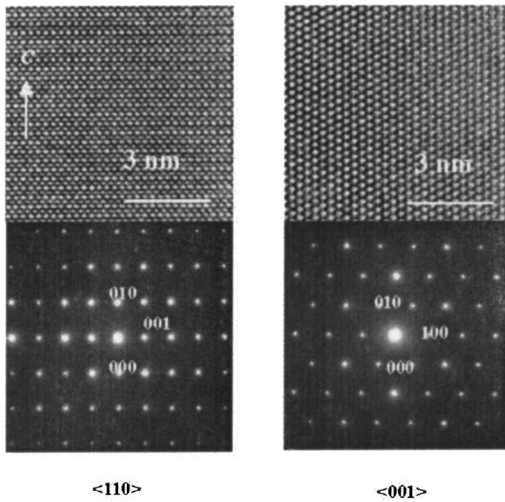


FIG. 2. Electron diffraction patterns and HRTEM images of a MgB₂ single crystal for beam directions of [110] and [001] in the hexagonal structure.

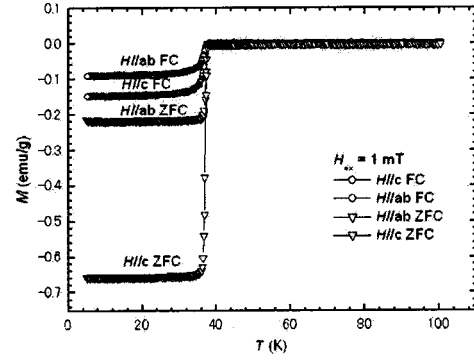


FIG. 3. Temperature dependent magnetization curves for the MgB₂ single crystal. FC and ZFC denote the field cooling and zero field cooling curves, respectively.

plane view of the high resolution transmission electron microscope (HRTEM) images and electron diffraction patterns in selected areas for beam directions of [110] and [001], as shown in Fig. 2, which indicated an atomic arrangement with the $P6/mmm$ cell of MgB₂. From the left hand side of Fig. 2, we recognize two kind of layers with different spot sizes alternately stacking along the c axis. Neither extra spots nor streaks were found, indicating that the crystal is of high quality.

III. ANISOTROPY OF THE UPPER CRITICAL FIELD

The temperature dependence of the magnetization curve was measured at 1 mT along the c axis and the ab plane by a superconducting quantum interference device magnetometer. Figure 3 represent the results of magnetization measurements for the MgB₂ single crystal. It shows the $M(T)$ curves in the zero-field-cooling and field-cooling modes. The onset of superconducting transition was obtained at $T_c=38$ K, with transition widths $\Delta T_c=0.8$ K both for $H\parallel ab$ and for $H\parallel c$, indicating the high quality of the samples, where $\parallel ab(\parallel c)$ denotes the field H perpendicular (parallel) to the c axis, respectively. The transition temperatures are slightly lower than T_c of polycrystalline specimens (≈ 39 K), as well as those of single crystals described in previous results.^{15,17,18,24} The suppression of T_c was considered to be due to impurity contamination from container materials (BN, Mo, and Nb). In order to check the contamination, we per-

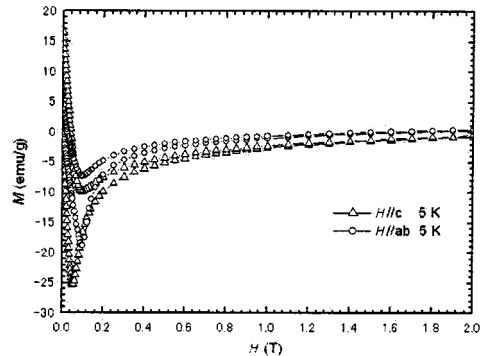


FIG. 4. The magnetic hysteresis curves $M(H)$ at 5 K.

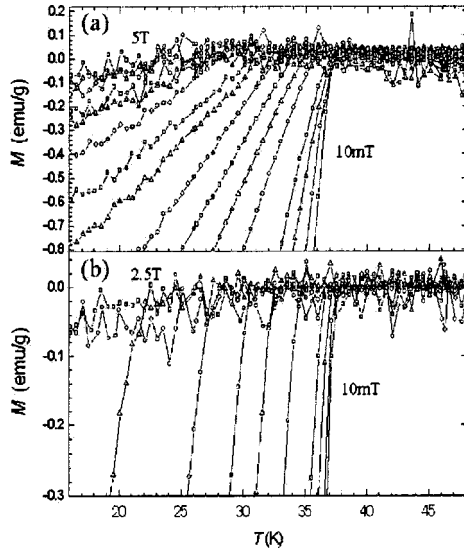


FIG. 5. Temperature dependence of the magnetization on zero-field cooling in several fields for (a) $H\parallel ab$ and (b) $H\parallel c$.

formed a qualitative analysis by an electron probe microanalyzer (EPMA). As a result, no contamination from our container elements (Mo, Fe, Ni, and Co) was detected within a 0.1% accuracy.

Figure 4 shows the magnetic hysteresis curves $M(H)$ at 5 K for applied fields up to 2 T for $H\parallel ab$ and for $H\parallel c$, indicating the characteristic curve of type-II superconductors with very small hysteresis loops. This implies that the single crystal has slight pinning effects, indicating pure single crystals with high quality.

Figure 5 shows the temperature dependence of magnetization $M(T)$ curves on warming after field cooling of the sample for (a) $H\parallel ab$ in a magnetic field up to 5 T and (b) $H\parallel c$ in a magnetic field up to 2.5 T. The superconducting transition shifts to lower temperatures as the field is increased. The superconducting transition temperatures in finite fields are determined by extrapolating the negative part of the $M(T)$ curve linearly and by finding the crossing point to the horizontal line extended from the normal state. Using this criterion, the upper critical fields of MgB_2 for applied fields $H\parallel ab$ and $H\parallel c$ are obtained, as shown in Fig. 6(a). It

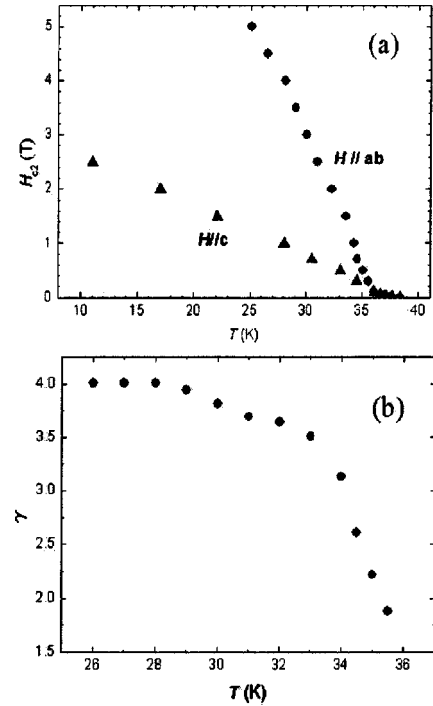


FIG. 6. (a) Upper critical field for H_{c2}^{ab} and H_{c2}^c determined from the onset of the superconductivity in Figs. 5(a) and 5(b) as a function of the temperature. H_{c2}^{ab} reveals a positive curvature, while H_{c2}^c has a linear temperature dependence. (b) Temperature dependence of the upper critical field anisotropy $\gamma = H_{c2}^{ab}/H_{c2}^c$.

is seen that H_{c2}^{ab} shows a positive curvature in the temperature dependence near T_c , and then rises rapidly at lower temperatures. In contrast, H_{c2}^c increases linearly with decreasing temperature. These temperature dependences of H_{c2} have also been observed in MgB_2 single crystals by Lyard *et al.*²³ and were thought to be a characteristic feature of layered superconductors such as NbSe_2 .²⁶ Therefore, the anisotropy ratio $\gamma = H_{c2}^{ab}/H_{c2}^c$ is found to be temperature dependent, as displayed in Fig. 6(b). It increases from about 1 near T_c to 4.0 at 25 K. The extrapolation of H_{c2}^{ab} and H_{c2}^c lines to the zero temperature axis yields $H_{c2}^{ab}(0) \sim 13.6$ T and $H_{c2}^c(0) \sim 3.4$ T, with $\gamma \sim 4.0$. Using the Ginzburg-Landau equation $H_{c2} = \Phi_0 / (2\pi\xi^2)$, the coherence lengths ξ were

TABLE II. Comparison of physical parameters with single crystals prepared by different methods.

Parameter	Our sample	References 21, 19, and 24	References 15 and 25	M. Xu <i>et al.</i> (Ref. 18)	References 17, 20, and 23
a (Å)	3.0863(4)	3.085(1)	3.0851(5)	3.047(1)	3.09 ± 0.06
c (Å)	3.5178(4)	3.518(2)	3.5201(5)	3.404(1)	
R	0.020	0.015–0.020	0.018		
R_w	0.027	0.015–0.020	0.025		
T_c (K)	38	38–39	38.1–38.3	39	38
$H_{c2}^{ab}(0)$ (T)	13.6	14.5, ^a 23 ^b	21–22	19.8	17
$H_{c2}^c(0)$ (T)	3.4	3.18, ^a 3.1 ^b	7.0–7.5	7.7	3.5
γ (T)	1(T_c)-4.0(25 K)	1(T_c)-4.2(22 K), ^a 2.8(35 K)-6(15 K) ^b	2.2(T_c)-3(30 K)	2.6(0 K)	2(T_c)-4.4(22 K)

^aValues determined from the magnetic measurement.

^bValues determined from the magnetic torque measurement.

yielded to be $\xi_{ab}(0) \sim 10$ nm and $\xi_c(0) \sim 3$ nm. These values are similar to the previous results obtained from magnetic measurements on powder samples²⁷ or on single crystals^{19–23} and the values determined from the calculation using the two band model,²⁸ but do not agree with the reported γ -values determined from resistivity measurements on bulk samples^{15–18,10,11,29} and *c*-axis-oriented films,^{12–14} which are around 1.1 to 3, as shown in Table II.

IV. CONCLUSION

We have succeeded in synthesizing the single crystals under ambient pressure. So far the single crystals were produced by using special high pressure facilities. The synthesized single crystals are found to be of good quality ($R=0.020$, $R_w=0.027$) judging from the structural analysis

standard.

We measured the magnetic properties of single crystalline MgB₂, and found a marked anisotropy; H_{c2}^{ab} reveals a positive curvature while H_{c2}^c increases linearly in the temperature dependence. The anisotropy ratio $\gamma=H_{c2}^{ab}/H_{c2}^c$ of the upper critical field is shown to be increased from about 1 near T_c to 4.0 at 25 K.

ACKNOWLEDGMENTS

We would like to thank K. Yamawaki, K. Noda, K. Ishikawa, H. Saito, Y. Takano, and K. Ohshima for useful discussions. This work has been supported in part by the 21st century COE program under the Ministry of Education, Culture, Sports, Science and Technology.

*Corresponding author. FAX: +81-45-924-5339. Email address: machida@lipro.msl.titech.ac.jp

- ¹J. Nagamatsu, N. Nakagawa, T. Muranaka, Y. Zenitani, and J. Akimitsu, *Nature (London)* **410**, 63 (2001).
- ²S. L. Bud'ko, G. Lapertot, C. Petrovic, C. E. Cunningham, N. Anderson, and P. C. Canfield, *Phys. Rev. Lett.* **86**, 1877 (2001).
- ³J. W. Quilty, A. Yamamoto, and S. Tajima, *Phys. Rev. Lett.* **88**, 087001 (2002).
- ⁴J. Kortus, I. I. Marzin, K. D. Belashchenko, V. P. Antropov, and L. L. Boyer, *Phys. Rev. Lett.* **86**, 4656 (2001).
- ⁵A. Y. Liu, I. I. Marzin, and J. Kortus, *Phys. Rev. Lett.* **87**, 087005 (2001).
- ⁶F. Bouquet, R. A. Fisher, N. E. Phillips, D. G. Hinks, and J. D. Jorgensen, *Phys. Rev. Lett.* **87**, 047001 (2001).
- ⁷P. Szabó, P. Samuely, J. Kačmarčík, T. Klein, J. Marcus, D. Fruchart, and S. Miraglia, *Phys. Rev. Lett.* **87**, 137005 (2001).
- ⁸F. Giubileo, D. Roditchev, W. Sacks, R. Lamy, D. X. Thanh, and J. Klein, *Phys. Rev. Lett.* **87**, 177008 (2001).
- ⁹M. Iavarone, G. Karapetrov, A. E. Koshelev, W. K. Kwok, G. W. Crabtree, and D. G. Hinks, *cond-mat/0203329* (unpublished).
- ¹⁰F. Simon *et al.*, *Phys. Rev. Lett.* **87**, 047002 (2001).
- ¹¹O. F. de Lima, R. A. Ribeiro, M. A. Avila, C. A. Cardoso, and A. A. Coelho, *Phys. Rev. Lett.* **86**, 5974 (2001).
- ¹²S. Patnaik *et al.*, *Supercond. Sci. Technol.* **14**, 315 (2001).
- ¹³M. H. Jung, M. Jaime, A. H. Lacerda, G. S. Boebinger, W. N. Kang, H. J. Kim, E. M. Choi, and S. I. Lee, *Chem. Phys. Lett.* **343**, 447 (2001).
- ¹⁴R. J. Olsson *et al.*, *cond-mat/0201022* (unpublished).
- ¹⁵S. Lee, H. Mori, T. Masui, Y. Eltsev, A. Yamamoto, and S. Tajima,

J. Phys. Soc. Jpn. **70**, 2255 (2001).

- ¹⁶A. K. Pradhan, Z. X. Shi, M. Tokunaga, T. Tamegai, Y. Takano, K. Togano, H. Kito, and H. Ihara, *Phys. Rev. B* **64**, 212509 (2001).
- ¹⁷K. H. P. Kim *et al.*, *Phys. Rev. B* **65**, 100510 (2002).
- ¹⁸M. Xu, H. Kitazawa, Y. Takano, J. Ye, K. Nishida, H. Abe, A. Matsushita, N. Tsujii, and G. Kido, *Appl. Phys. Lett.* **79**, 2779 (2001).
- ¹⁹M. Angst, R. Puzniak, A. Wisniewski, J. Jun, S. M. Kazakov, J. Karpinski, J. Roos, and H. Keller, *Phys. Rev. Lett.* **88**, 167004 (2001).
- ²⁰U. Welp *et al.*, *cond-mat/0203337* (unpublished).
- ²¹M. Zehetmayer, M. Eisterer, H. W. Weber, J. Jun, S. M. Kazakov, J. Karpinski, and A. Wisniewski, *cond-mat/0204199* (unpublished).
- ²²A. V. Sologubenko, J. Jun, S. M. Kazakov, J. Karpinski, and H. R. Ott, *Phys. Rev. B* **65**, 180505 (2002).
- ²³L. Lyard *et al.*, *cond-mat/0206231* (unpublished).
- ²⁴J. Karpinski *et al.*, *cond-mat/0207263* (unpublished).
- ²⁵Y. Eltsev, S. Lee, K. Nakao, N. Chikumoto, S. Tajima, N. Koshizuka, and M. Murakami, *cond-mat/0202133* (unpublished).
- ²⁶K. Takanaka, *J. Phys. Soc. Jpn.* **52**, 2173 (1983).
- ²⁷S. L. Bud'ko and P. C. Canfield, *cond-mat/0201085* (unpublished).
- ²⁸P. Miranović, K. Machida, and V. G. Kogan, *cond-mat/0206231* (unpublished).
- ²⁹G. K. Perkins, J. Moore, Y. Bugoslavsky, L. F. Cohen, J. Jun, S. M. Kazakov, J. Karpinski, and A. D. Caplin, *cond-mat/0205036* (unpublished).